ApoB-75, a truncation of apolipoprotein B associated with familial hypobetalipoproteinemia: genetic and kinetic studies

Elaine S. Krul, Klaus G. Parhofer, P. Hugh R. Barrett,* R. Doug Wagner, and Gustav Schonfeld

Lipid Research Center, Washington University School of Medicine, 4566 Scott Avenue, Box 8046, St. Louis, MO 63110, and Resource Facility for Kinetic Analysis, Center for Bioengineering,* University of Washington, Seattle, WA 98195

Abstract We have identified a mutation of apolipoprotein B (apoB) in a kindred with hypobetalipoproteinemia. Four affected members had plasma concentrations of total cholesterol of 115 ± 14, low density lipoprotein (LDL)-C of 48 ± 11, and apoB of 28 ± 9 (mg/dl mean ± SD). The values correspond to ~30% the values for unaffected relatives. Triglyceride and high density lipoprotein (HDL)-C concentrations were 92 ± 50 and 49 ± 4, respectively, neither significantly different from unaffected relatives. Western blots of plasma apoB of affected subjects showed two major bands: apoB-100 and an apoB-75 (mol wt of ~418,000). DNA sequencing of the appropriate polymerase chain reaction (PCR)-amplified genomic DNA segment revealed a deletion of the cytidine at nucleotide position 10366, resulting in a premature stop codon at amino acid residue 3387. In apoB-75/apoB-100 heterozygotes, two LDL populations containing either apoB-75 or apoB-100 could be distinguished from each other by gel permeation chromatography and by immunoblotting of nondenaturing gels using monoclonal antibodies B1B3 (epitope between apoB amino acid residues 3506–3635) and C1.4 (epitope between residues 97–526). ApoB-75 LDL were smaller and more dense than apoB-100 LDL. To determine whether the low concentration of apoB-75 was due to its enhanced LDL-receptor-mediated removal, apoB-75 LDL were isolated from the proband's d 1.063–1.090 g/ml fraction (which contained most of the apoB-75 in his plasma) by chromatography on anti-apoB and anti-apoA-I immunoaffinity columns. The resulting pure apoB-75 LDL fraction interacted with the cells 1.5-fold more effectively than apoB-100 LDL (d 1.019–1.063 g/ml). To determine the physiologic mechanism responsible for the hypobetalipoproteinemia, in vivo kinetic studies were performed in two affected subjects, using endogenous labeling of apoB-75 and apoB-100 with [^{13}C]leucine followed by multicompartmental kinetic analyses. Fractional catabolic rates of apoB-75 VLDL and LDL were 2- and 1.3-fold those of apoB-100 very low density lipoprotein (VLDL) and LDL, respectively. Production rates of apoB-75 were ~30% of those for apoB-100. This differs from the behavior of apoB-89, a previously described variant, whose FCRs were also increased ~1.5-fold relative to apoB-100, but whose production rates were nearly identical to those of apoB-100. Thus, in contrast to the apoB-89 mutation, the apoB-75 mutation imparts two physiologic defects to apoB-75 lipoproteins that account for the hypobetalipoproteinemia, diminished production and increased catabolism. —**Krul, E. S., K. G. Parhofer, P. H. R. Barrett, R. D. Wagner, and G. Schonfeld.** ApoB-75, a truncation of apolipoprotein B associated with familial hypobetalipoproteinemia: genetic and kinetic studies. *J. Lipid Res.* 1992. **33:** 1037–1050.

Supplementary key words apolipoprotein B • genetics • kinetic models • cholesterol • LDL production • hypobetalipoproteinemia • [^{13}C]leucine • LDL-receptor • LDL-catabolism • apoB-75

ApoB-100 and apoB-48 are the naturally occurring forms of apoB in plasma. In humans, apoB-100 consisting of 4536 amino acids is synthesized in liver and secreted as an integral protein of VLDL particles. ApoB-48 is translated, in intestinal enterocytes, from apoB-100 mRNAs that are edited to produce a stop codon at amino acid position 2153, and is secreted with chylomicrons (1). In addition to these natural forms, a subgroup of individuals with low cholesterol concentrations and familial hypobetalipoproteinemia also produce unusual truncated forms of apoB that cosegregate with the hypobetalipoproteinemia in affected members of kindreds (2–11). Natural mutations giving rise to truncated forms of apoB varying in size from apoB-9 to apoB-89 have been described. Various sized apoB molecules also have been expressed in cultured cells transfected with engineered vectors (12–14). Studies of both the naturally inherited and engineered truncations are beginning to provide important information on the structure–function relations of apoB, for functions such as lipid binding, lipoprotein assembly, and cell recognition.

Abbreviations: LDL, low density lipoproteins; HDL, high density lipoproteins; PCR, polymerase chain reaction; IDL, intermediate density lipoproteins; VLDL, very low density lipoproteins; PMSF, phenylmethylsulfonylfluoride; IPB, immunoprecipitation buffer; LPDS, lipoprotein-deficient serum; RFLP, restriction fragment length polymorphism; I/D, insertion/deletion; GC–MS, gas chromatography–mass spectrometry; FCR, fractional catabolic rate; GGE, gradient gel electrophoresis; VNTR, variable number of tandem repeats.

In this communication we report a new truncation of apoB, apoB-75, and describe the molecular defect, haplotype, lipoprotein distribution, cell recognition, and in vivo kinetics of this truncated form of apoB. It was anticipated that this study would provide information on the function of the carboxyl 25% of apoB-100. Moreover, it was expected that the comparison between apoB-75 and the previously reported apoB-89 would reveal some characteristics of the 653 amino acid long region between apoB-75 and apoB-89.

METHODS

Blood collection and plasma analyses

The proband was identified through screens of blood donors obtained from the St. Louis Red Cross Blood Bank, volunteers at community screening, and patients undergoing coronary artery catheterization as previously described (15, 16). Blood cells were separated by low speed centrifugation from fasting blood samples. Leukocytes were immediately isolated from packed blood cells using Histopaque-1077 (Sigma Chemical Co., St. Louis, MO) and stored at −20°C prior to DNA isolation (see below). Total plasma lipids were determined in the Washington University Lipid Research Center Core Laboratory using protocols of the Lipid Research Clinics (17).

For the in vivo kinetic studies, blood was drawn according to the study protocol outlined below. Plasma was processed immediately for isolation of lipoproteins and aliquots were stored at −70°C until analysis.

Isolation of lipoproteins

VLDL plus intermediate density lipoprotein (IDL) (d<1.019 g/ml), LDL (d 1.019–1.063 g/ml), and HDL (d 1.063–1.21 g/ml) were isolated by sequential ultracentrifugation unless otherwise indicated (18). Protease inhibitors (20 μM D-phe-L-phe-L-arg chloromethylketone (PPACK) and 20 μM D-phe-L-pro-L-arg chloromethylketone (Pierce Chemical Co., Rockford, IL) and antibiotics (0.1 mg/ml gentamicin) were added to the plasmas prior to ultracentrifugation as previously described (2). Lipoprotein fractions were dialyzed against EDTA/saline, pH 8, at 4°C and were generally used immediately after isolation. Lipoprotein subfractions were prepared by immunoaffinity chromatography using columns with monoclonal antibodies of defined specificities as previously described (19) with the exception that a desalting column was not attached in series to the affinity columns. Lipoproteins specifically bound and eluted from the affinity columns were immediately dialyzed against EDTA/saline, pH 8. Protein mass in each lipoprotein fraction was determined by the method of Lowry et al. (20).

For the kinetic studies, VLDL (d<1.006 g/ml), IDL (d 1.006–1.019 g/ml), and LDL (d 1.019–1.090 g/ml) were isolated by sequential ultracentrifugation (18) from 4 ml of plasma using a 50.4 TI rotor (Beckman Instruments Inc., Palo Alto, CA).

FPLC separation of plasma

Plasma (1.5 ml) was chromatographed on two 25-ml Superose 6 columns at room temperature as described previously (2). The column eluent was analyzed enzymatically for cholesterol (Wako Pure Chemicals, Richmond, VA). Equal aliquots (35 μl) were removed from each column fraction and applied to 3–6% gradient SDS-PAGE gels for electrophoresis and immunoblotting (described below). Bands corresponding to apoB-100 and apoB-75 on the resulting autoradiograph were scanned using a laser densitometer. Areas under the peaks were determined using SigmaScan (Jandel Scientific, Corte Madera, CA).

Electrophoresis and immunoblotting

Electrophoresis of plasma on 3–6% gradient SDS-PAGE gels was performed as described previously (2) with the exception that apoB was immunoprecipitated from plasma prior to electrophoresis. Briefly, Triton X-100 was added to plasma to a final concentration of 1%. Two volumes of immunoprecipitation buffer (IPB) (20 mM PBS, pH 7.4, 0.15 M NaCl, 5 mM EDTA, 1% Triton X-100, 0.5% sodium deoxycholate, 0.1% SDS) were added, followed by 0.5 volume of a polyclonal anti-human apoB antibody (R197-4) in 1% Triton X-100 and 50 μg/ml PMSF. Samples were mixed by gentle tapping and allowed to incubate overnight at 4°C. Two volumes of a 10% solution of Staph A cells (Immuno-Precipitin, Bethesda Research Laboratories, Gaithersburg, MD) were added, followed by gentle mixing. The samples were incubated at room temperature for 1 h with occasional mixing after which the immunoprecipitates were separated by centrifugation. Pellets were washed twice with IPB and dissolved in SDS-PAGE sample buffer, boiled, and applied to 3–6% gradient SDS polyacrylamide gels for electrophoresis.

Nondenaturing gradient gel electrophoresis of whole plasma and isolated lipoprotein fractions was performed according to the method of Krauss and Burke (21). Electrotransfer of proteins separated on polyacrylamide gels was performed essentially as described by Towbin, Staehelin, and Gordon (22) with the exception that for nondenaturing gels methanol was omitted from the transfer buffer. Immunoblotting with anti-apoB monoclonal antibodies was carried out as described previously (2).

DNA preparation

Genomic DNA was isolated from leukocytes by the method of Davis, Dibner, and Battey (23). The DNA was resuspended in sterile H_2O and stored at 4°C.

Polymerase chain reaction and DNA sequencing

A pair (B75-A, B75-B) of oligonucleotides (20 nucleotides) was synthesized by automated procedures by the Protein Chemistry Core Facility at Washington University Medical School as PCR amplification primers for the region suspected to contain the mutation (**Fig. 1**). The 5' amplification primer started at cDNA position 10201 and the 3' amplification started at cDNA position 10710 according to the sequence of Knott et al. (24). The 510 nucleotide PCR product contained an internal *Pst* I site near the 5 9r end and an internal *Eco* RI site near the 3' end. Five μg of genomic DNA and 0.5 pmol of each 5' and 3' primer were amplified in 100-μl reactions with recombinant *Taq* polymerase as reported previously (25).

For sequencing, genomic DNA was amplified by 30 cycles of PCR at 95°C for 30 sec, 55°C for 30 sec, and 72°C for 3 min, purified with GeneClean (Bio 101, La Jolla, CA), and digested with *Pst* I and *Eco* RI. The resulting cohesive ends were ligated into the polylinker region of M13mp18. *E. coli* JM109 cells were transformed with the recombinant bacteriophage and 20 colorless plaques were picked to obtain single-stranded recombinant M13 DNA to use as sequencing templates. DNA was sequenced by the Sequenase dideoxy sequencing procedure (United States Biochemical Corp., Cleveland, OH) (26).

Allele-specific oligonucleotide analyses

A pair of allele-specific oligonucleotides (ASO) was synthesized with the following sequences: B75-WT, 5'-AAGCTCACAGTACTGTTAT-3'; B75-MUT, 5'-AAGCTCACATACTGTTAT-3'. The oligonucleotides were 5' end-labeled with [^{32}P]ATP (ICN Biomedicals, Inc., Costa Mesa, CA) using T4 polynucleotide kinase (Boehringer Mannheim, Indianapolis, IN) to a specific radioactivity of 0.1 μCi/pmol. Twenty μl of each 100 μl PCR product was denatured by the addition of NaOH to a final concentration of 0.2 N. The mixture was heated to 95°C for 5 min and quenched with 400 μl of ice-cold 15× SSC. Two hundred-μl aliquots were applied to two GeneScreen membranes on a slot-blot apparatus. The membranes were baked at 80°C for 2 h and prehybridized for 18 h at 42°C in 6× SSC, 0.1% SDS, and 10× Denhardt's. The membranes were hybridized with either the wild type or mutant ASO for 24 h at 42°C after which the membranes were washed twice with 6× SSC, 0.1% SDS for 5 min at room temperature and once for 5 min at 55°C. The membranes were air-dried and exposed to Kodak XAR-5 film for 2 h at −70°C using intensifying screens.

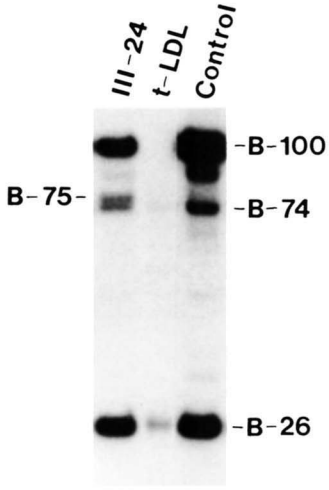

Fig. 1. Identification of the apoB-75 protein. Immunoprecipitated apoB from the plasma of the proband (III-24) and an unrelated control subject were run on a 3–6% SDS-PAGE gel. Thrombin-digested LDL apoB-100 (t-LDL) was applied to the center lane to identify the positions of apoB-74 and apoB-26. Immunoblotting with an anti-apoB monoclonal antibody (C1.4) was performed as described in Methods. The resultant autoradiograms are shown with the apoB species as determined by molecular weights indicated. The apoB-100 in the plasma samples shown has undergone some proteolytic degradation. These are shown to indicate the relative migration of apoB-75.

RFLP, VNTR and insertion/deletion analyses

Oligonucleotide pairs were used as PCR primers to amplify the fragments of the subjects' DNA containing the *Apa* LI, *Alu* I, *Hinc* II, *Pvu* II, *Xba* I, *Msp* I, and *Eco* RI RFLP sites of the apoB gene (27). A pair of oligonucleotides were used to amplify the 5' region of the apoB gene containing the insertion/deletion (I/D) polymorphism of the signal peptide sequence, as described previously (28). An additional oligonucleotide pair was used to amplify the 3' region of the apoB gene containing the VNTR sequences at the 3' end of exon 29 (29).

DNA amplifications, restriction endonuclease digestion, and agarose gel evaluations were all performed as described previously (15). Amplification primers for the Hinc II RFLP were synthesized with the following sequences: *Hinc* II-1, 5'-CTAACCATCTCTGAGCAAAATATCC-3'; *Hinc* II-2, 5'-GTTGGCATGCACACGTTTCAGCCAC-3'. PCR amplification, digestion of the purified PCR product, and the rest of the *Hinc* II RFLP analysis was performed with the same parameters and procedures described for the *Xba* I RFLP (30). The *Apa* LI and the *Alu* I RFLP analyses were performed as per Young et al. (6) and Wang et al. (31), respectively.

Lipoprotein binding by cultured human fibroblasts

LDL binding and degradation assays with human fibroblast cultures were performed as previously described (2). Fibroblasts were grown in culture dishes and experiments were begun after incubation in lipoprotein-deficient serum (LPDS) for 48 h. Competitor lipoproteins were added to the cell cultures in media containing 10% LPDS simultaneously with a constant amount of ^{125}I-labeled control B-100 LDL. The ability of these preparations to inhibit the binding of ^{125}I-labeled control B-100 LDL to cells was compared at 4°C. Incubations of the

lipoproteins with cells were carried out for 4 h. Lipoprotein binding was determined after fibroblasts were washed and dissolved in 0.1 M sodium hydroxide, aliquots were counted for cell-associated radioactivity. Additional aliquots were taken to determine total cell protein. Nonspecific binding or cell association was determined as the amount of bound or cell-associated radioactivity after incubation of ^{125}I-labeled LDL in the presence of at least a 50-fold excess of nonlabeled homologous lipoprotein.

In vivo kinetics of lipoproteins containing apoB-75 and apoB-100

Study protocol. The clinical characteristics of the two heterozygotes (III-24, IV-41) participating in the kinetic study are shown in **Table 1**; both were healthy and taking no medications. Details of the procedure for the kinetic studies have been published previously (32). In brief, the subjects did not change their regular diet 10 days prior to or throughout the 110-h study period. After subjects had fasted for 10 h, a primed constant infusion of [1-^{13}C]leucine (MSD Isotopes, Montreal, Canada, isotopic purity 99%) was started, consisting of a bolus (0.85 mg/kg), immediately followed by an 8-h constant infusion (at 0.85 mg/kg per h) of the tracer. After the infusion was stopped the subjects remained fasting for another 8 h. Forty-two samples of plasma were drawn for assays of amino acid enrichment (every 5 min during the first h and thereafter every 15 min, later half-hourly and hourly and finally daily up to 92 h). Thirty-two samples were drawn for VLDL-, IDL-, LDL-apoB leucine enrichment (every 10 min during the first h thereafter every 15 min, later half-hourly, hourly and finally every other day up to 92 h). Aliquots for determination of VLDL-, IDL-, and LDL-apoB pool sizes were drawn on five occasions during the course of the study.

Analytical methods. ApoB-75 and apoB-100 were separated by polyacrylamide gel (3–6%) electrophoresis (33) at each time point from each lipoprotein fraction. Aliquots corresponding to 50–100 μg of total protein were applied per lane. Coomassie blue-stained bands of apoB-75 and apoB-100 were excised and hydrolyzed in 12 N HCl for 16 h at 110°C. VLDL and IDL samples used for the gas chromatography–mass spectrometry (GC–MS) analyses had no or barely detectable amounts of apoB-26, indicating little proteolytic degradation of apoB-100, while LDL samples tended to have small amounts. The potential contamination of the apoB-75 with apoB-74 derived from apoB-100 in these samples would only tend to minimize any differences in kinetic parameters between apoB-75 and apoB-100, rather than magnify them. Amino acids were isolated from the hydrolyzed gel pieces or from 0.3 ml plasma by cation exchange chromatography (AG50W-X8, Bio-Rad, Richmond, CA) and derivatized to n-acetyl-n-propanol-esters (34). Enrichments were determined by GC–MS (35) and subsequently converted to tracer/tracee ratios as previously described (36).

TABLE 1. Clinical characteristics of the B-75 kindred

Subject	Sex	Age	BMI	TCHOL	TG	LDL-C	HDL-C	ApoB	ApoB Phenotype
		yr	*kg/m²*			*mg/dl*			
II-5	F	69	21.0	127	86	57	53	36	100/75
II-7	M	67	27.7	116	164	38	45	34	100/75
III-24[a,b]	M	46	28.7	96	52	40	46	15	100/75
IV-41[b]	M	27	24.4	122	65	58	51	28	100/75
Mean ± SD		52 ± 20	25.5 ± 3.5	115 ± 14[c]	92 ± 50	48 ± 11[d]	49 ± 4	28 ± 9[e]	
II-1	F	72	23.7	240	124	151	64	123	100/100
II-4	M	70	27.4	243	203	161	41	177	100/100
II-8	F	66	20.6	191	124	98	68	68	100/100
III-25	F	45	29.8	185	318	88	33	92	100/100
III-26	M	39	24.9	179	95	116	44	73	100/100
III-27	F	33	43.3	165	153	89	45	77	100/100
III-29	F	33	19.9	196	110	114	60	93	100/100
IV-43	F	25	21.8	165	89	74	73	52	100/100
IV-45	F	10	19.9	161	71	93	54	53	100/100
Mean ± SD		44 ± 22	25.7 ± 7.4	192 ± 31	143 ± 76	109 ± 30	54 ± 14	90 ± 3	

Plasma lipid profiles were determined using protocols of the Lipid Research Clinics. Plasma concentrations of apoB were determined by an established radioimmunoassay (except II-1 and II-4 which were determined by immunonephelometry). ApoB phenotypes were assigned on the basis of Western blotting analyses. BMI, body mass index; TCHOL, total plasma cholesterol; TG, total plasma triglyceride; LDL-C, LDL cholesterol; HDL-C, HDL cholesterol; ApoB, apolipoprotein B.

[a] Proband.

[b] Subjects in whom in vivo kinetic studies were performed.

[c] $P < 0.001$ (unpaired t-test) compared to B100/B100 phenotype.

[d] $P < 0.005$.

[e] $P < 0.01$ (Mann-Whitney Two Sample Test).

ApoB levels were measured in VLDL, IDL, and LDL fractions by radioimmunoassay (37) and concentrations were confirmed by protein assays (20). The values for apoB concentration measured with the radioimmunoassay did not differ by more than 20% from values estimated from the protein assay, assuming that approximately 40% of VLDL protein, 70% of IDL protein, and 90% of LDL protein represented apoB. Separation of apoB-75 from apoB-100 was achieved using 3–6% gradient SDS-polyacrylamide gels stained with Coomassie Blue. The protein bands corresponding to apoB-100 and apoB-75 were scanned by laser densitometry on an LKB Model 2202 Ultrascan (Bromma, Sweden). Areas under the peaks corresponding to apoB-100 and apoB-75 were quantitated using the program SigmaScan (Jandel Scientific, Corte Madera, CA). Based on the assumption that both forms of apoB have the same chromogenicity, pool sizes of apoB-75 and apoB-100 were estimated by scanning three to five samples from different time points in each lipoprotein fraction and averaging the ratios.

Kinetic analysis. A simple multicompartmental model was used to describe VLDL-, IDL-, and LDL-apoB leucine tracer/tracee ratios. This model has been shown to describe apoB metabolism in four normolipidemic controls (32) and is derived from previously published models (38–41). The model (shown in Fig. 10) consists of a precursor compartment (compartment 1) and an intracellular delay compartment accounting for the synthesis of apoB and the assembly of lipoproteins (compartment 2). Compartments 11 and 12 are used to account for the kinetics of the VLDL-apoB fraction and represent a minimal delipidation chain. IDL-apoB (compartment 21) can be derived from either of the two VLDL compartments. LDL-apoB (compartment 31) is derived from the IDL fraction (compartment 21) or directly from VLDL compartment 11 through a shunt pathway. It is assumed that plasma leucine (compartment 1) is the source of the leucine that is incorporated into apoB. Plasma leucine tracer/tracee ratio curves were similar to those noted and described earlier (32). A tri-exponential function (32) was used to fit the plasma leucine tracer/tracee ratios and was used as a forcing function (42) in the model. It is further assumed that all apoB enters the plasma via compartment 11, thus transport rates through compartment 11 correspond to total apoB production. In this study the CONSAM/SAAM (43) programs were used to fit the model to the observed tracer data. Metabolic parameters for apoB-100 and apoB-75 are subsequently derived from the best fit. The fractional catabolic rate (FCR) of VLDL-apoB is the weighted average (related to mass distribution) of the FCRs of pools 11 and 12. The FCR of each VLDL pool is the sum of individual rate constants (for compartment 11, rate constants relating to the following metabolic pathways: 11→12, 11→21, 11→31, and 11→out; for compartment 12, rate constants relating to 12→21 and 12→ out). The FCR of LDL-apoB corresponds to the rate of irreversible loss from compartment 31 (31→out). The only difference from the previously published model (32) is that a direct loss from compartment 11 (11→out) was required to fit the observed tracer/tracee ratios of VLDL-apoB-75. Because of the low mass of IDL-apoB-75, tracer/tracee ratios could not be determined in subject III-24. To fit the model in this subject it was therefore assumed that 50% of the IDL apoB-75 was converted to the LDL fraction. Changing the fraction of apoB-75 IDL converted to LDL from 0% to 100% does not significantly alter the VLDL to LDL conversion rates. Furthermore, the FCR of the IDL compartment was free to adjust to provide the delay necessary to fit the LDL data.

RESULTS

The proband and his kindred

The proband is a 46-year-old man, (Subject III-24 in Table 1 and Fig. 1) in good health, with total and LDL-

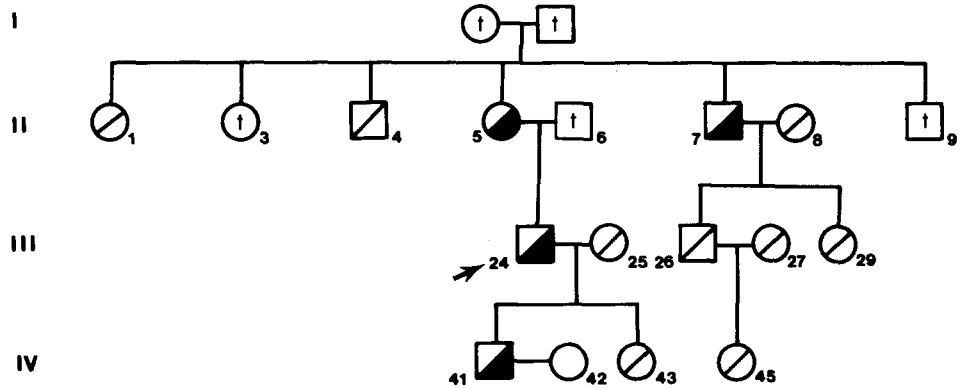

Fig. 2. Pedigree of the apoB-75 kindred. The proband is identified by an arrow. ApoB genotypes of the immediate family members were determined by Western blot analyses: ○, □, not sampled; ⊘, ⊠, B100/B100; ◔, ◪, B100/B75; †, deceased. Plasma lipids and apoB concentrations are given in Table 1.

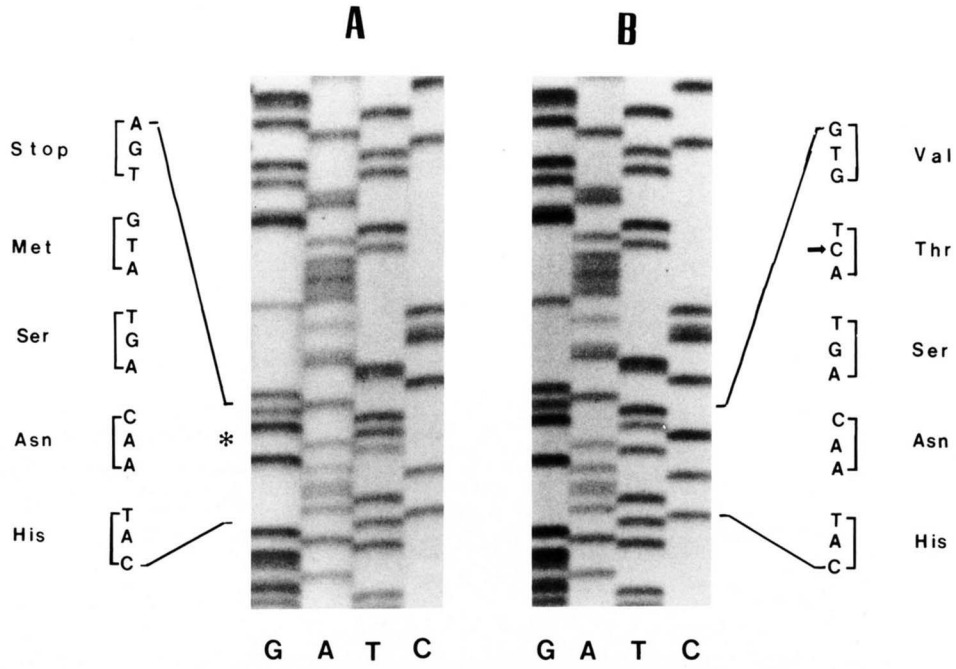

Fig. 3. Identification of the apoB-75 mutation. A pair of oligonucleotides (B75-3, B75-5) was synthesized as PCR amplification primers for the region suspected to contain the mutation responsible for the apoB-75 genotype (Fig. 1). Five μg of genomic DNA of subject III-24 (Table 1) and 0.5 pmol of each 5' and 3' primer were amplified in 100 μl reactions with recombinant *Taq* polymerase; 30 cycles at 95°C for 30 sec, 55°C for 30 sec, and 72°C for 3 min. Amplified DNA was purified, digested with *Pst* I and *Eco* RI and the resulting cohesive ends were ligated into the polylinker region of M13mp18. *E. coli* JM109 cells were transformed with the recombinant bacteriophage and 20 clones (colorless plaques) were picked to obtain single-stranded recombinant M13 DNA to use as sequencing templates. DNA was sequenced by the Sequenase dideoxy sequencing procedure (United States Biochemical Corp., Cleveland, OH). Seven of the clones yielded the mutant sequence shown here.

cholesterol and total apoB concentrations $<$5th percentile for his age, race, and gender. A medical history physical examination, routine chemistry screen, blood counts, and urinalysis were normal, ruling out any secondary causes of low LDL. An unusual apoB, apoB-75, was identified in his plasma by immunoblotting (Fig. 1). His mother, maternal uncle, and son also had total LDL-cholesterol and total apoB concentrations that were significantly lower than those of nonaffected relatives, and the apoB-75 truncation cosegregated with low LDL and apoB concentrations (**Fig. 2**, Table 1).

The apoB-75 mutation

The appropriate region of genomic DNA, determined from the size of the apoB truncation, was amplified by PCR using the primers and procedures described in the Methods section. The PCR products were ligated into the M13 mp18 vector which was then used to obtain single-stranded DNA clones for sequencing. Ten clones were sequenced of which three yielded the "wild type" sequence. Seven clones contained a cytidine deletion in nucleotide position 10366, altering codon 3386 from ACT(Thr) to ATG(Met) and codon 3387 from GTC(val) to TGA(stop) (**Fig. 3**). The 3386 amino acids of this apoB represent 74.7% of the 4536 amino acids contained in apoB-100. Allele-specific nucleotides were used to identify other affected members of the kindred. There was a perfect

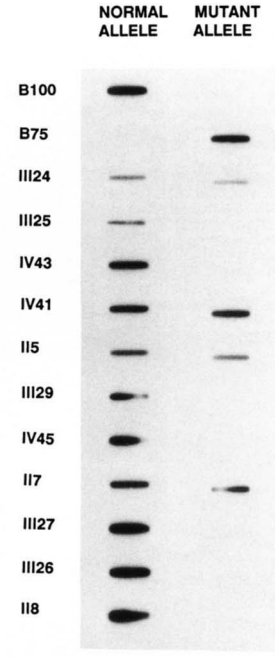

Fig. 4. Allele-specific oligonucleotide analysis. A pair of allele-specific oligonucleotides (ASO) for apoB-100 (normal allele) and apoB-75 (mutant allele) were synthesized as described in Methods. The ASO analysis was performed as described and the resultant autoradiograms are shown. Control plasmids containing the appropriate apoB-100 or apoB-75 sequences were used as controls and are indicated at the top of the autoradiogram. Samples of DNA used for PCR are identified by the donor according to the numbering system used for the pedigree (see Fig. 2).

TABLE 2. Haplotype markers of B-75 kindred

Subject	Haplotype	SP	*Apa* L1	*Hinc* II	*Pvu* II	*Alu* I	*Xba* I	*Msp* I	*Eco* RI	VNTR
III 24[a]	79/91	−/−	+/+	−/−	−/+	+/+	+/−	+/+	+/+	37/47
III 25	199/79	+/−	+/+	−/−	−/−	−/+	+/+	+/+	+/+	37/37
IV 43	199/91	+/−	+/+	−/−	−/+	−/+	+/−	+/+	+/+	37/47
IV 41[a]	199/79	+/−	+/+	−/−	−/−	−/+	+/+	+/+	+/+	37/37
II 5[a]	199/79	+/−	+/+	−/−	−/−	−/+	+/+	+/+	+/+	37/39
III 29	79/77	−/−	+/+	−/−	−/−	+/+	+/+	+/−	+/+	37/37
IV 45	79/69	−/−	+/+	−/−	−/−	+/−	+/+	+/−	+/+	37/37
II 7[a]	79/79	−/−	+/+	−/−	−/−	+/+	+/+	+/+	+/+	37/37
III 27	79/5	−/−	+/−	−/−	−/−	+/−	+/+	+/−	+/+	33/37
III 26	79/69	−/−	+/+	−/−	−/−	+/−	+/+	+/−	+/+	33/37
II 8	69/77	−/−	+/+	−/−	−/−	−/+	+/+	−/−	+/+	33/37
		2^7	2^6	2^5	2^4	2^3	2^2	2_1	2^0	

The haplotype numbers in the second column were determined by using the binary system for the eight RFLP markers according to the method described by Ludwig et al. (27). A minus sign (−) denotes 0 and a plus sign (+) denotes 1. Thus, − for all markers would be haplotype 0 (absence of restriction sites) and + for all markers would be haplotype 255 (all eight diallelic sites contain the restriction sites). The bottom line illustrates how each marker is assigned to a particular binary number. Assignments of +/− versus −/+ were made on the basis of segregation analyses within the B-75 kindred.

[a]The apoB-75 phenotype was associated with haplotype 79.

cosegregation in the kindred between the genetic defect and the protein truncation (**Fig. 4**). Haplotypes were constructed using the markers, methods, and binary system described by Ludwig and McCarthy (27) (**Table 2**). Phase was assigned by segregation analysis of the kindred. Each of the affected individuals had at least one allele 79 (calculated according to the method of Ludwig et al. (27) and described in the legend to Table 2), but not all kindred members with allele 79 carried the apoB-75 mutation. The cosegregation of the protein and gene defects and of haplotypes makes it very likely the C deletion is indeed responsible for the truncation, although definitive proof would require expression of the protein in a cell culture system.

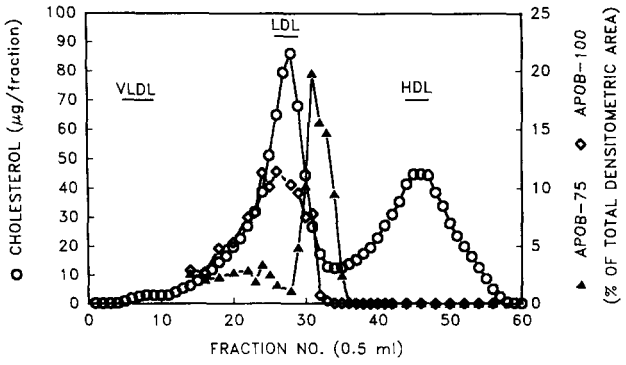

Fig. 5. Separation of plasma apoB-100 from apoB-75. Plasma (1.5 ml) was chromatographed on two 25-ml gel permeation Superose 6 columns at room temperature. Column buffer consisted of 0.15 M NaCl, 1 mM EDTA, pH 8. The elution of proteins was monitored by absorbance at 280 nm and the initial 12 ml was diverted to waste. The subsequent eluent was collected in 60 0.5-ml fractions. The column eluent was analyzed for cholesterol enzymatically (Wako Pure Chemicals, Richmond, VA). Equal aliquots (35 μl) were removed from fractions 14–60 and applied to 3–6% gradient SDS-PAGE gels for electrophoresis. The separated proteins were electrotransferred to nitrocellulose. The blots were incubated with MAb C1.4 as described for the nondenaturing gels in Fig. 6. Bands corresponding to apoB-100 and apoB-75 on the resultant autoradiograph were scanned using a laser densitometer. Areas under the peaks were determined using SigmaScan (Jandel Scientific, Corte Madera, CA). The areas under the peaks corresponding to either apoB-100 or apoB-75 were summed and the values provided represent percents of the total densitometric area determined for any particular fraction. The peak of the apoB-100 immunoreactivity eluted between fractions 24–26 whereas the peak of apoB-75 immunoreactivity eluted at fraction 31, corresponding to a smaller sized LDL particle.

ApoB-75 in plasma

To ascertain the lipoprotein distribution of apoB-75, the plasma of the proband was fractionated by *a)* gel exclusion chromatography (**Fig. 5**), *b)* nondenaturing polyacrylamide gel electrophoresis (GGE) (**Fig. 6**), and *c)* sequential ultracentrifugation (**Fig. 7**). Chromatographic fractions eluted from two Superose 6 columns were analyzed for cholesterol, apoB-100, and apoB-75. Cholesterol eluted in three major fractions corresponding to VLDL, LDL, and HDL (Fig. 5). ApoB-100 (detected by SDS-polyacrylamide gel electrophoresis) was present in VLDL, IDL, and exhibited a major peak corresponding to the LDL cholesterol fraction. ApoB-75 was also present in VLDL and IDL, but the major apoB-75 peak in LDL was retarded relative to apoB-100 LDL and clearly separated from it, suggesting that two populations of LDL may have been present, one containing apoB-100 and the other apoB-75. The presence of two LDL populations was confirmed by GGE analysis of several plasmas of affected individuals and controls (Fig. 6). On immunoblotting of the GGE gel with MAb C1.4 (epitope, amino acid residues 97–526) (44), two populations of LDL were visible in apoB-75/apoB-100 heterozygotes (Fig. 6). In addition, the two populations of LDL were also separable from each other by sequential ultracentrifugation. When density fractions were separated on the GGE gels, apoB-100 and apoB-75 LDL were both present in the d 1.019–1.063 g/ml range (Fig. 6), but only the smaller of the two popu-

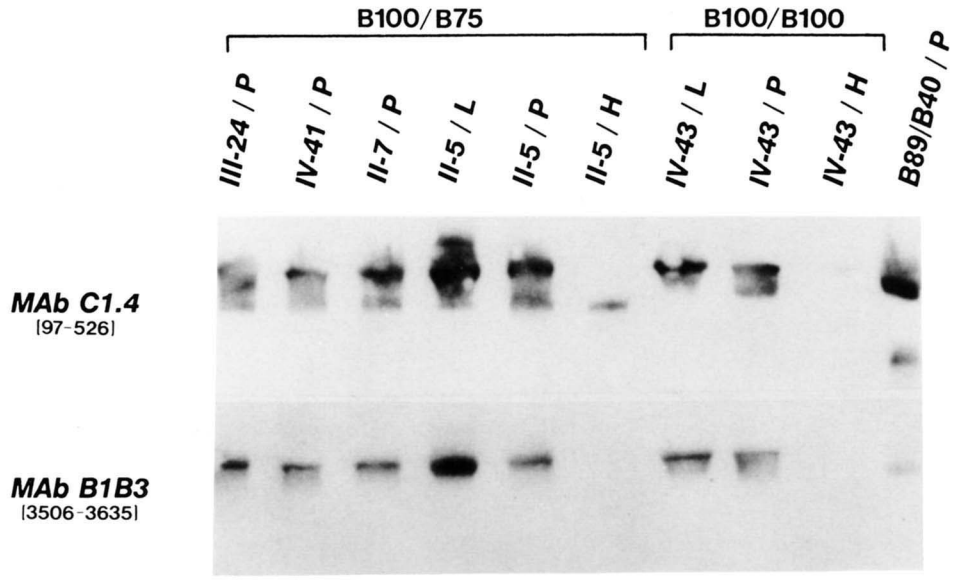

Fig. 6. Separate apoB-75 and apoB-100 LDL particles detected by Western blot analysis of nondenaturing gradient gels. Plasma (P), (20 μl) or 20 μg of LDL (1.019–1.063 g/ml) (L) or HDL (1.063–1.21 g/ml) (H) from the indicated kindred members were electrophoresed on 2–16% gradient nondenaturing polyacrylamide gels. Two replicate gels were run. After electrophoresis was complete the separated lipoproteins were electrotransferred from the gel to nitrocellulose in transfer buffer lacking methanol. Immunoblotting with MAbs C1.4 and B1B3 was performed as described in Methods. The resultant autoradiographs are shown. MAb C1.4 directed towards the amino terminal amino acids 97–526 of apoB-100 reacts with two populations of particle sizes in the plasmas and LDL fractions of kindred members having B100/B75 genotypes. In the HDL fraction of subject II-5 only the smaller of the two particles appeared to be present. A control lane containing plasma from a B89/B40 heterozygote revealed immunoreactivity of two lipoprotein species with MAb C1.4. In the replicate immunoblot incubated with MAb B1B3, only the larger of the two particle populations was immunoreactive in the B100/B75 heterozygotes. As the B1B3 epitope lies beyond the apoB-75 termination site, only the apoB-100 immunoreactive particles were visualized. No apoB-100 was detected in the HDL fraction of subject II-5, therefore the particles reactive with MAb C1.4 contained exclusively apoB-75.

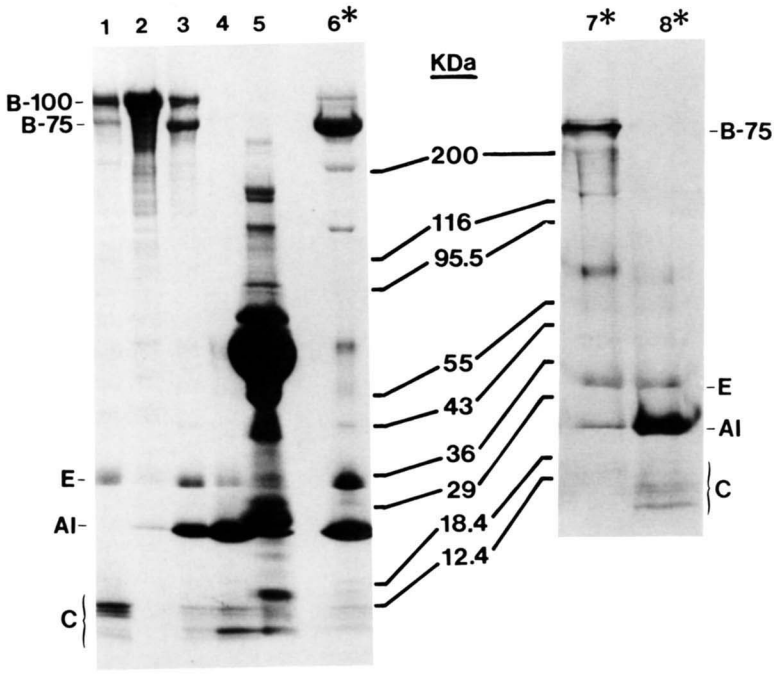

Fig. 7. Purification of apoB-75 monitored by Coomassie-blue stained gradient 3–15% SDS-PAGE gels of III-24 lipoproteins. Lipoproteins were isolated from III-24 plasma by ultracentrifugation at the following densities: <1.019 g/ml (lane 1), 1.019–1.063 g/ml (lane 2), 1.063–1.090 g/ml (lane 3), 1.090–1.124 g/ml (lane 4), and d>1.124 g/ml (lane 5). Approximately 30 μg of lipoprotein protein was electrophoresed in each lane, except lane 5. Lanes 6, 7, and 8 correspond to lipoprotein fractions isolated after affinity chromatography and are indicated with an *. Density 1.063–1.090 g/ml fraction from III-24 plasma was applied onto the B1B3 affinity column. The flow-through (FT) fraction is shown in lane 6. This fraction contains essentially no apoB-100, is enriched in apoB-75, but contains substantial amounts of apoA-I and apoE indicating contamination with HDL. Another preparation of d 1.063–1.090 g/ml lipoprotein was applied onto the B1B3 column and the flow-through fraction was applied onto an anti-apoA-I column. The flow-through (FT) and retained (RET) fractions are shown in lanes 7 and 8, respectively. The FT fraction is enriched in apoB-75 and is depleted of apoA-I and apoE. The RET fraction has no apoB and is enriched with apoA-I, apoE, and apoCs.

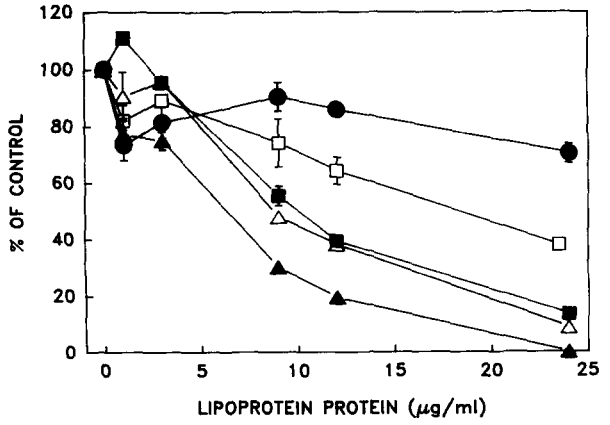

Fig. 8. Fibroblast 4°C LDL binding inhibition assay using affinity isolated lipoproteins. A constant amount of control ^{125}I-labeled B-100/B-100 LDL (d 1.019–1.063 g/ml) was added to each well with or without increasing concentrations of homologous LDL (■), homologous d 1.063–1.090 g/ml lipoprotein (●), proband LDL (△), or affinity-isolated lipoproteins from the proband. The affinity-isolated apoB-75 LDL corresponding to lane 7 in Fig. 7 which lacks apoB-100 is indicated by a ▲. The HDL fraction corresponding to lane 8 in Fig. 7 is indicated by a □. Proband (III-24) LDL (B-100/B-75) did not complete significantly more effectively than B-100/B-100 LDL for radiolabeled LDL binding to the LDL receptor on fibroblasts. The B-100/B-100 d 1.063–1.090 g/ml fraction competed least effectively. However, the affinity-isolated apoB-75-LDL and depleted of HDL competed 1.5 times better than B-100/B-100 LDL for binding when expressed on a molar basis; the apoB-75 LDL still competed 1.2 times more effectively than apoB-100 LDL.

lations was seen in the d 1.063–1.090 g/ml fractions (Fig. 6, lane II-5/H). When MAb B1B3 (epitope residues, 3506– 3635) (44) was used, only one population of LDL was seen corresponding to LDL-apoB-100. No MAb B1B3-reactive material was seen in the d 1.063–1.21 g/ml fraction (lane II-5/H) suggesting that only the smaller population of particles corresponding to LDL-apoB-75 was present in that higher density range.

Upon ultracentrifugation, apoB-75 was found to be present in the d<1.019 g/ml, and d 1.019–1.063 g/m fractions (Fig. 7) but the relative proportions of apoB-75 to apoB-100 appeared to be greater in the d 1.063–1.090 g/ml fraction than in either less dense fraction, confirming the gel filtration profiles (Fig. 5).

Interactions of apoB-75 LDL with the LDL-receptor

As the relative amounts of apoB-75 appeared to be greatest in the d 1.063–1.090 g/ml fraction, this fraction was used as starting material for the isolation of apoB-75 LDL. The first step consisted of immunoaffinity chromatography on an MAb B1B3-containing column that retained apoB-100 LDL and allowed apoB-75 LDL to flow through, along with some apoE- and apoA-I-containing HDL particles (Fig. 7, lane 6). To remove the HDL particles, the MAb B1B3 flow-through fraction was applied to an anti-apoA-I immunoaffinity column. The flow-through fractions of this latter column contained predominantly LDL-apoB-75 (Fig. 7, lane 7) and the retained fractions lacked apoB-75 and contained predominantly apoA-I and apoE. Most of density and immunoaffinity isolated fractions competed with normal ^{125}I-labeled LDL for binding to cultured normal fibroblasts (**Fig. 8**). The most active fraction (ED_{50} ~6 μg/ml) was the one containing only apoB-75 LDL (isolated from the proband, III-24), followed by the d 1.019–1.063 g/ml LDL fractions isolated from a normal control subject and the proband (ED_{50} ~10 μg/ml). The LDL (d 1.019–1.063 g/ml) of the control subject contained only apoB-100, while the proband LDL (d 1.019–1.063 g/ml) contained mostly apoB-100 and small amounts of apoB-75. (The ratio of apoB-75 to apoB-100 based on absorbance of bands in Coomassie blue-stained polyacrylamide gels was ~1:15).

In vivo kinetics of lipoproteins containing apoB-75 and apoB-100

To confirm the cell culture studies and to determine what other kinetic mechanism accounted for the hypobetalipoproteinemia in this kindred, tracer studies were performed in two apoB-75/apoB-100 heterozygotes.

The concentrations of apoB in VLDL, IDL, and LDL and the percent of apoB-75 in each fraction determined during the kinetic study are shown in **Table 3**. (ApoB values shown in Table 1 were obtained upon the initial screening of plasma samples and may not correspond exactly to the values obtained on the day of the kinetic experiments.) With increasing density fractions the percentage of apoB-75 in the lipoproteins decreased (17% in VLDL to 7% in LDL). ApoB concentrations and the ratio of apoB-75/apoB-100 remained constant throughout the study period, indicating that the subjects remained in a steady state.

Fig. 9 shows VLDL (panel A) and LDL (panel B) apoB leucine tracer/tracee ratios plotted versus time for subject

TABLE 3. Distribution of apoB in VLDL, IDL, and LDL

	VLDL		IDL		LDL	
Subject	mg/dl	% ApoB-75	mg/dl	% ApoB-75	mg/dl	% ApoB-75
III-24	3.8 ± 1.1	17.4 ± 1.5	1.5 ± 0.7	9.1 ± 1.3	16.1 ± 0.9	6.2 ± 1.0
IV-41	2.9 ± 0.3	16.4 ± 2.0	2.9 ± 0.4	8.1 ± 1.1	15.9 ± 1.1	7.7 ± 0.7

ApoB-75 contents in the lipoprotein fractions were determined for three to five samples according to the procedures described in the Methods section. The values here correspond to the mean values ± SD obtained.

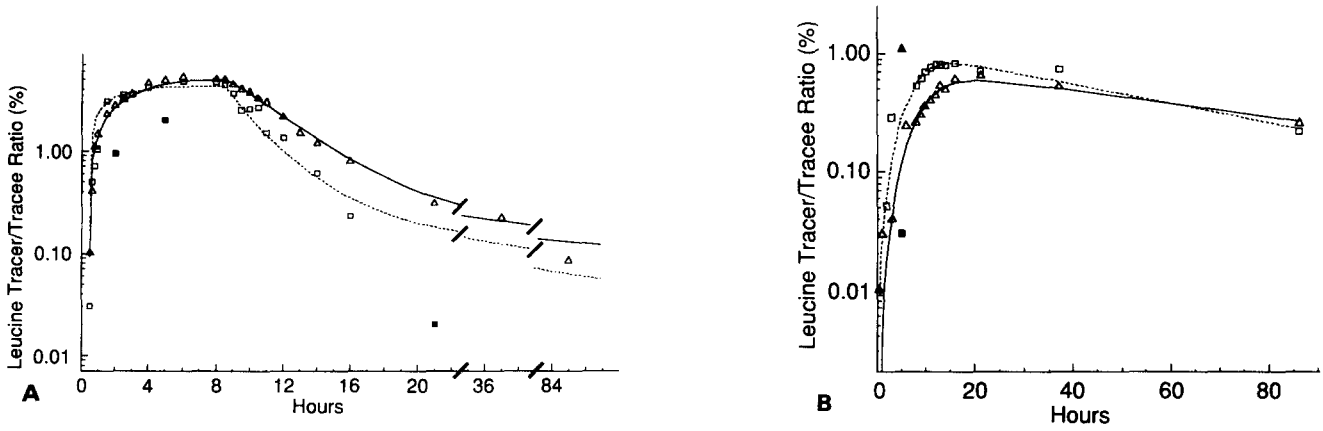

Fig. 9. ApoB-75- and apoB-100-leucine tracer/tracee ratio versus time curves for VLDL and LDL. Observed values for apoB-100 (△) and apoB-75 (□) and respective calculated fits (—) and (---) to the VLDL-(A) and LDL-apoB(B) tracer/tracee ratio data, using the multicompartmental model in subject IV-41. Solid symbols represent data points excluded from the fitting process.

IV-41. Symbols represent observed values while lines represent best fits of the multicompartmental model (**Fig. 10**) to the tracer data. As can be seen in Fig. 9, there is good agreement between the model-derived fits and the observed apoB-75 and apoB-100 tracer data. The lag time before the appearance of labeled apoB-75 and apoB-100 in the VLDL fraction was approximately 0.5 h for both proteins. Both the upward and the downward slopes of the tracer/tracee ratio curves for VLDL-apoB-75 were steeper than the corresponding slopes for VLDL-apoB-100 and "plateau" values were reached earlier for the tracer/tracee ratios of the truncated protein (panel A). In the LDL fraction (panel B) the slopes of the tracer/tracee ratio curves were also slightly steeper for the apoB-75 than for apoB-100 particles, and the tracer/tracee ratios in LDL-apoB-75 curves peaked at somewhat higher values than in the LDL-apoB-100 curves. The differences in upward and downward slopes, together with the earlier "plateau" in VLDL and the higher peaks in LDL represent increased rates of appearance and disappearance of labeled apoB-75 compared to labeled apoB-100-containing lipoproteins.

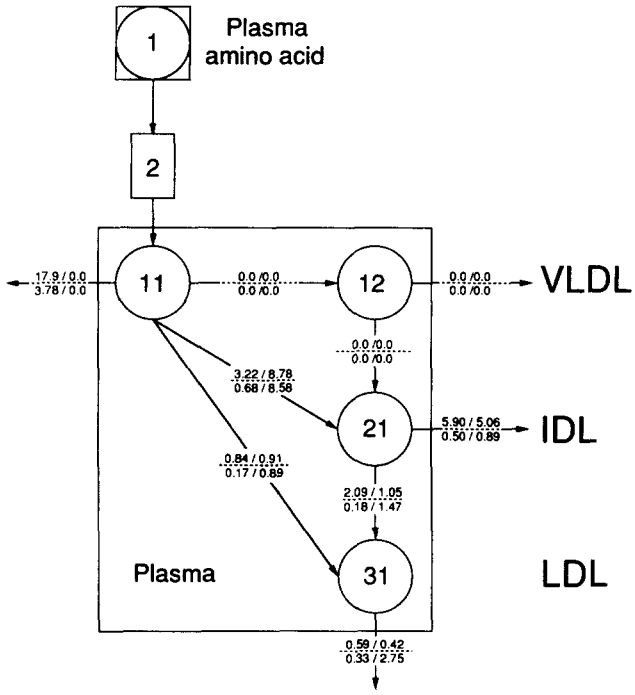

Fig. 10. Multicompartmental model describing the metabolism of apoB in VLDL: compartments 11 and 12; IDL: compartment 22; and LDL: compartment 31. The values above dotted lines represent rate constants (pools/day); those values below the lines represent transport rates (mg/kg/day) along individual metabolic pathways. The values to the left of the slash refer to apoB-75 and those on the right refer to apoB-100.

While the qualitative differences between the kinetics of apoB-75 and apoB-100 can be appreciated from the figures directly, multicompartmental modeling is necessary to quantify these differences (Fig. 10). **Table 4A and B** show metabolic parameters for apoB-75 and apoB-100 derived by multicompartmental modeling. The FCRs of VLDL and LDL apoB-75 were 1.3–2 times higher than those of apoB-100 (Table 4A). ApoB-75 production rates were only one-third of those for apoB-100 (Table 4B). Table 4B also shows the percent of VLDL apoB converted to LDL apoB. The conversion of apoB-75-containing VLDL is only 20–30% that of the apoB-100-containing particles. This suggests that the increased FCR of apoB-75 reflects an enhanced irreversible loss of particles from each lipoprotein fraction rather than an increased conversion of VLDL to LDL. Thus, less apoB-75 ultimately reached the LDL fraction as compared to apoB-100. The greater selective losses of apoB-75 from VLDL are also evident from the fact that with increasing particle density the percent of apoB-75 mass relative to apoB-100 mass decreased (Table 3).

In Fig. 10 all rate constants as well as all transport rates

TABLE 4. Kinetic parameters estimated by multicompartmental analysis

	A				B			
	VLDL FCR		LDL FCR		ApoB Production		VLDL-LDL Conversion	
Subject	ApoB-75	ApoB-100	ApoB-75	ApoB-100	ApoB-75	ApoB-100	ApoB-75	ApoB-100
	pools/day		*pools/day*		*mg/kg/day*		%	
III-24	18.5 ± 1.9	9.1 ± 0.4	0.62 ± 0.17	0.50 ± 0.06	5.5 ± 0.6	11.6 ± 0.5	3.6 ± 1.9[a]	21.0 ± 2.5
IV-41	21.9 ± 1.9	9.7 ± 0.5	0.59 ± 0.05	0.42 ± 0.05	4.6 ± 0.4	9.5 ± 0.5	7.6 ± 0.5	24.9 ± 2.9

Parameters were determined using the multicompartmental model described in Fig. 10. Values represent best estimates ± SD. FCR, fractional catabolic rate.

[a]This value is based on the assumption that 50% of apoB-75 IDL is converted to LDL as outlined in Methods.

are presented for subject IV-41. Note that the rate constants of all removal pathways are higher for apoB-75 than for apoB-100. It is also interesting that in one of the two subjects a slowly turning over VLDL compartment was not required to fit the tracer data. Also, in the second subject (data not shown) the mass of apoB transported through this compartment was low. This figure furthermore reveals that a considerable amount of apoB-75 is removed directly from the fast turning over VLDL compartment (compartment 11), while no such pathway was required to fit the apoB-100 data. This is in accordance with our results in normolipidemic control subjects, in whom also no such direct removal pathway was required to fit the data (32).

DISCUSSION

ApoB-75 is a heretofore undescribed truncation of apoB coinherited with hypobetalipoproteinemia. The genetic defect consists of a deletion of the cytosine in nucleotide position 10366 that produces a stop codon in residue position 3385 (Fig. 3), resulting in the synthesis and secretion of a protein 74.7% of its full length, namely apoB-75 according to the centile system (45). The mutation is associated with decreases of LDL-cholesterol and apoB concentrations to ~30% of those seen in unaffected relatives (Table 1). Both apoB-100 and apoB-75 are distributed among VLDL- and LDL-sized particles with the majority of apoB-75 being associated with a small, dense LDL (Figs. 5 and 6). However, apoB-75 accounted for about 17% of the total apoB protein in VLDL and only about 7% of the total apoB protein in LDL (Table 3).

Fifteen other unique truncations are known to exist in humans ranging from apoB-9 to apoB-89, and the various truncated proteins are distributed differently among the major size and/or density classes of lipoproteins in fasting plasma (1–11). The shortest, apoB-9, apoB-25, and apoB-29, are not detectable in plasma, apoB-31 is present almost exclusively in the HDL density range, and apoB-37, apoB-39, and apoB-40 are found in all density classes but mostly in HDL; apoB-46, apoB-50, apoB-54.8, apoB-55, and apoB-67 are found in VLDL and LDL but mostly in VLDL; apoB-75, apoB-83, apoB-87, and apoB-89 are found primarily in LDL but also in VLDL. The absence of apoB-25 and apoB-29 from plasma is probably due to very slow secretion from liver and/or intestine or due to very rapid degradation or both. It is probably not due to the complete absence of any secretion because even shorter pieces are secreted by cells transfected with the appropriate vectors (e.g., apoB-13, consisting of 583 amino acids) (46). The switchover from exclusively HDL-like to some VLDL-like particles between apoB-31 and apoB-37 suggests that residues 1425 to 1728 importantly alter the composition and metabolism of apoB-containing particles. Similar arguments can be made for the regions between apoB-40 and apoB-54.8 (amino acid residues 1829 to 2485) and apoB-67 and apoB-83 (amino acid residues 3040 to 3749) each of which is associated with a change in the density distribution of apoB-containing particles. For most of the mutations, it is unknown which biochemical-metabolic processes are affected. Thus, it is unclear whether changes in biosynthesis, intracellular assembly, secretion, intravascular conversion, or clearance are associated with these altered distributions in plasma. So far, kinetic studies have only been performed for apoB-89 (15), apoB-50 (47), and apoB-75 described here.

ApoB-75 LDL are bound to cultured fibroblasts with greater affinity than apoB-100 LDL (Fig. 8). This finding, similar to that reported for apoB-89 and apoB-87, highlights the importance of the carboxyl terminal region of apoB-100 beyond apoB-75 (residue 3387). This segment is distal to the putative LDL-receptor recognition region (residues 3167–3297) yet its deletion appears to enhance the binding of the mutant LDL particles to the LDL-receptor, suggesting a role for this distant region in the modulation of receptor binding. However, at this point the authors cannot rule out a possible role of apoE in mediating the enhanced binding of this particle to the LDL receptor.

The implication of the enhanced LDL-receptor binding of apoB-75 is that apoB-75 VLDL and/or LDL particles may be cleared more rapidly from plasma than apoB-100 particles. Indeed the kinetic studies performed

in two heterozygous subjects support that conclusion (Figs. 9 and 10). The kinetic analysis, however, is based on several assumptions. First, the subjects are in steady state with respect to their apoB metabolism. Indeed, plasma apoB concentrations in individual lipoprotein fractions throughout the study period remained constant. Second, apoB-75 and apoB-100 are located on different lipoprotein molecules but the metabolic pathways they follow are similar, i.e., secretion as VLDL, conversion to IDL and LDL. Indeed, apoB-75 is found in lipoproteins similar in density to the fractions containing apoB-100, and several lines of evidence clearly show that apoB-100 and apoB-75 are on distinct particles. Third, the multicompartmental model correctly describes the metabolism of apoB-75 and apoB-100. As previously described (32), apoB-100 metabolism in normolipidemic subjects is adequately described with this model. A minor modification, namely the addition of a removal pathway from the fast turning over VLDL compartment, was required to fit the model to the apoB-75 data presented here. While this model may be an oversimplification of true apoB metabolism, our conclusions are largely "model-independent", as they are drawn from comparisons of apoB-75 kinetic parameters to those for apoB-100 obtained in the same person under identical conditions. Fourth, pool sizes of apoB-75 and apoB-100 were estimated on the assumption that both proteins have the same chromogenicity. While it has been shown that apoB-48 differs in this respect from apoB-100 (48), this is unknown for apoB-75. However, the differences between the chromogenicities of apoB-100 and apoB-75 are likely to be smaller than the differences between apoB-100 and apoB-48. To the extent that estimated pool sizes are incorrect, calculated production rates may be slightly over- or underestimated.

The kinetic analysis shows that apoB levels are low in these subjects due to a decreased apoB production and an increased FCR of apoB-75-containing particles. It is unknown at which step(s) in the production scheme (i.e., mRNA stability, translation, intracellular degradation, particle assembly and secretion) the production of apoB-75 containing lipoproteins is impaired. However, there is growing evidence that not all of newly synthesized apoB-100 is secreted. In fact, a substantial fraction of newly synthesized apoB is degraded intracellularly (49, 50). It is possible that the fraction of intracellular degradation is significantly increased in the case of an abnormal apolipoprotein due either to faulty assembly of lipoprotein particles or the absence of appropriate targeting mechanisms for secretion. The increased FCR of VLDL and LDL particles containing the truncated apolipoprotein could reflect enhanced binding of apoB-75 lipoproteins to the LDL-receptor due to differences in the conformations of apoB. It is also possible that the apoE contents or apoE/apoC ratios of these particles are altered, thereby affecting VLDL clearance rates. Whatever the mechanism, the fibroblast experiments (Fig. 8) indicate that the increased FCR of apoB-75 LDL is at least partially mediated through an increased binding to the LDL receptor. The enhanced LDL-receptor binding of smaller LDL particles is compatible with the lattice model of LDL-receptor-LDL interactions proposed by Chappell et al. (51).

Comparison of kinetic parameters found in this study with those published for normolipidemic control subjects may explain, at least in part, why apoB-100 particles are present at ~30% rather than the expected 50% of normal concentrations. The production rate of apoB-100 in the heterozygotes is not grossly abnormal, but the fraction of VLDL apoB-100 converted to LDL appears to be relatively low compared with normals (32), indicating that the apoB-100 VLDL particles in our heterozygotes may be preferentially cleared from plasma rather than being converted to LDL. This could result in the lower than expected concentrations of apoB-100 VLDL and LDL particles. By which factors this increased clearance of apoB-100 VLDL particles is regulated and by which mechanism it is mediated are not clear. One possibility could be an upregulation of LDL-receptors due to low plasma cholesterol concentrations; however, in the current study the FCRs for apoB-100 LDL were normal (Table 4).

It is instructive to compare the apoB-75 defect with the apoB-89 defect. With respect to density and size distribution in plasma, and enhanced recognition and clearance by the LDL-receptor, apoB-75 particles resemble the previously reported apoB-89 lipoproteins, but there is one notable difference. While apoB-89 and apoB-100 are produced at nearly the same rate in apoB-89/apoB-100 heterozygotes, apoB-75 is produced at a much reduced rate compared with apoB-100 in apoB-75/apoB-100 heterozygotes (Table 4). Thus, while apoB-89 is present in reduced concentrations primarily because of its enhanced FCR, apoB-75 is present in reduced concentrations relative to apoB-100 for two reasons; a reduced production rate and an enhanced FCR.

The authors acknowledge the expert technical assistance of Julie Dunn, Tish Kettler, and Tom Kitchens. The authors are grateful to DT, the proband, and his family for their helpful cooperation, to the staff of the General Clinical Research Center at Washington University, and to Diana Tessereau for scheduling visits. Cheryl Doyon prepared the manuscript. These studies were funded by NIH grants 5R01-HL42460, RR002176, and HL30086. Klaus G. Parhofer is a Fellow of the American Heart Association, Missouri Affiliate.

Manuscript received 6 January 1992 and in revised form 13 March 1992.

REFERENCES

1. Young, S. G. 1990. Recent progress in understanding apolipoprotein B. *Circulation.* **82:** 1574–1594.
2. Krul, E. S., M. Kinoshita, P. Talmud, S. E. Humphries,

S. Turner, A. C. Goldberg, K. Cook, E. Boerwinkle, and G. Schonfeld. 1989. Two distinct truncated apolipoprotein B species in a kindred with hypobetalipoproteinemia. *Arteriosclerosis.* **9:** 856–868.
3. Talmud, P., L. King-Underwood, E. S. Krul, G. Schonfeld, and S. Humphries. 1989. The molecular basis of truncated forms of apolipoprotein B in a kindred with compound heterozygous hypobetalipoproteinemia. *J. Lipid Res.* **30:** 1773–1779.
4. Young, S. G., S. J. Bertics, L. K. Curtiss, and J. L. Witztum. 1987. Characterization of an abnormal species of apolipoprotein B, apolipoprotein B-37, associated with familial hypobetalipoproteinemia. *J. Clin. Invest.* **79:** 1831–1841.
5. Young, S. G., S. J. Bertics, L. K. Curtiss, B. W. Dubois, and J. L. Witztum. 1987. Genetic analysis of a kindred with familial hypobetalipoproteinemia. Evidence for two separate gene defects: one associated with an abnormal apolipoprotein B species, apolipoprotein B-37; and a second associated with low plasma concentrations of apolipoprotein B-100. *J. Clin. Invest.* **79:** 1842–1951.
6. Young, S. G., S. T. Hubl, D. A. Chappell, R. S. Smith, F. Claiborne, S. M. Snyder, and J. F. Terdiman. 1989. Familial hypobetalipoproteinemia associated with a mutant species of apolipoprotein B (B-46). *N. Engl. J. Med.* **320:** 1604–1610.
7. Young, S. G., S. T. Hubl, R. S. Smith, S. M. Snyder, and J. F. Terdiman. 1990. Familial hypobetalipoproteinemia caused by a mutation in the apolipoprotein B gene that results in a truncated species of apolipoprotein B(B-31). A unique mutation that helps to define the portion of the apolipoprotein B molecule required for the formation of buoyant, triglyceride-rich lipoproteins. *J. Clin. Invest.* **85:** 933–942.
8. Young, S. G., S. T. Northey, and J. B. McCarthy. 1988. Low plasma cholesterol levels caused by a short deletion in the apolipoprotein B gene. *Science.* **241:** 591–593.
9. Collins, D. R., T. J. Knott, R. J. Pease, L. M. Powell, S. C. Wallis, S. Robertson, C. R. Pullinger, R. W. Milne, Y. L. Marcel, S. E. Humphries, P. J. Talmud, J. K. Lloyd, N. E. Miller, D. Muller, and J. Scott. 1988. Truncated variants of apolipoprotein B cause hypobetalipoproteinemia. *Nucleic Acids Res.* **16:** 8361–8375.
10. Huang, L-S., M. E. Ripps, S. H. Korman, R. J. Deckelbaum, and J. L. Breslow. 1989. Hypobetalipoproteinemia due to an apolipoprotein B gene exon 21 deletion derived by alu-alu recombination. *J. Biol. Chem.* **264:** 1394–1400.
11. Huang, L-S., H. Kayden, R. J. Sokol, and J. L. Breslow. 1991. ApoB gene nonsense and splicing mutations in a compound heterozygote for familial hypobetalipoproteinemia. *J. Lipid Res.* **32:** 1341–1348.
12. Graham, D. L., T. J. Knott, T. C. Jones, R. J. Pease, C. R. Pullinger, and J. Scott. 1991. Carboxyl-terminal truncation of apolipoprotein B results in gradual loss of the ability to form buoyant lipoproteins in cultured human and rat liver cell lines. *Biochemistry.* **30:** 5616–5621.
13. Yao, Z., B. D. Blackhart, M. F. Linton, S. M. Taylor, S. G. Young, and B. J. McCarthy. 1991. Expression of carboxyl-terminally truncated forms of human apolipoprotein B in rat hepatoma cells. *J. Biol. Chem.* **266:** 3300–3308.
14. Herscovitz, H., M. Hadzopoulou-Cladaras, M. T. Walsh, C. Cladaras, V. I. Zannis, and D. M. Small. 1991. Expression, secretion, and lipid-binding characterization of the N-terminal 17% of apolipoprotein B. *Proc. Natl. Acad. Sci. USA.* **88:** 7313–7317.
15. Parhofer, K. G., H. Barrett, D. M. Bier, and G. Schonfeld. 1991. Lipoproteins containing apoB-89 are cleared from human plasma more rapidly than apoB-100 lipoproteins. *Arteriosclerosis.* **11:** 1439a.
16. Wagner, R. D., E. S. Krul, J. Tang, K. G. Parhofer, K. Garlock, P. Talmud, and G. Schonfeld. 1991. ApoB-54.8, a truncated apolipoprotein found primarily in VLDL, is associated with a nonsense mutation in the apoB gene and hypobetalipoproteinemia. *J. Lipid Res.* **32:** 1001–1011.
17. Lipid Research Clinics Program. 1974. Manual of Laboratory Operations. Vol. 1. Lipid and Lipoprotein Analysis. DHEW Publication No. (NIH) 75-628. Washington, DC: US Government Printing Office.
18. Havel, R. J., H. A. Eder, and J. H. Bragdon. 1955. The distribution and chemical composition of ultracentrifugally separated lipoproteins in human serum. *J. Clin. Invest.* **34:** 1345–1353.
19. Krul, E. S., M. J. Tikkanen, and G. Schonfeld. 1988. Heterogeneity of apolipoprotein E epitope expression on human lipoproteins: importance for apolipoprotein E function. *J. Lipid Res.* **29:** 1309–1325.
20. Lowry, O. H., N. J. Rosebrough, A. L. Farr, and R. J. Randall. 1951. Protein measurement with the Folin phenol reagent. *J. Biol. Chem.* **193:** 265–275.
21. Krauss, R. M., and D. J. Burke. 1982. Identification of multiple subclasses of plasma low density lipoproteins in normal humans. *J. Lipid Res.* **23:** 97–104.
22. Towbin, H., T. Staehelin, and J. Gordon. 1979. Electrophoretic transfer of proteins from polyacrylamide gels to nitrocellulose sheets: procedure and some applications. *Proc. Natl. Acad. Sci. USA.* **76:** 4350–4354.
23. Davis, L. G., M. D. Dibner, and J. F. Battey. 1986. Methods in Molecular Biology. Elsevier, Amsterdam. 388.
24. Knott, T. J., R. J. Pease, L. M. Powell, S. C. Wallis, S. C. Rall, Jr., B. Blackhart, W. H. Taylor, Y. Marcel, R. Milne, T. L. Innerarity, M. Fuller, A. J. Lusis, B. J. McCarthy, R. W. Mahley, D. Johnson, J. Scott, and B. Levy-Wilson. 1986. Complete protein sequence and identification of structural domains of human apolipoprotein B. *Nature.* **323:** 734–738.
25. Saiki, R. K., D. H. Gelfand, S. Stoffel, S. J. Scharf, R. Higuchi, G. T. Horn, K. B. Mullis, and H. A. Erlich. 1988. Primer-director enzymatic amplification of DNA with a thermostable DNA polymerase. *Science.* **239:** 487–491.
26. Sanger, F., A. R. Coulson, and S. Nicklen. 1977. DNA sequencing with chain-termination inhibitors. *Proc. Natl. Acad. Sci. USA.* **74:** 5463–5467.
27. Ludwig, E. H., and B. J. McCarthy. 1990. Haplotype analysis of the human apolipoprotein B mutation associated with familial defective apolipoprotein B-100. *Am. J. Hum. Genet.* **47:** 712–720.
28. Boerwinkle, E., and L. Chan. 1989. A three codon insertion/deletion polymorphism in the signal peptide region of the human apolipoprotein B (apoB) gene directly typed by the polymerase chain reaction. *Nucleic Acids Res.* **17:** 4003.
29. Boerwinkle, E., W. Xiong, E. Fourest, and L. Chan. 1989. Rapid typing of tandemly repeated hypervariable loci by the polymerase chain reaction applications to the apolipoprotein B 3' hypervariable region. *Proc. Natl. Acad. Sci. USA.* **86:** 212–216.
30. Boerwinkle, E., S. S. Lee, R. Butler, V. N. Schumaker, and L. Chan. 1990. Rapid typing of apolipoprotein B DNA polymorphisms by DNA amplification. Association between Ag epitopes of human apolipoprotein B-100, a signal peptide insertion deletion polymorphism, and a 3' flanking DNA variable number of tandem repeats polymorphism of the apolipoprotein B gene. *Atherosclerosis.* **81:** 225–232.

31. Wang, X., P. Schlapfer, Y. Ma, R. Butler, J. Elovson, and V. N. Schumaker. 1988. Apolipoprotein B: The Ag (al/D) immunogenetic polymorphism coincides with a T-to-C substitution at nucleotide 1981, creating an alu-L restriction site. *Arteriosclerosis.* **8:** 429–435.
32. Parhofer, K. G., P. H. R. Barrett, D. M. Bier, and G. Schonfeld. 1991. Determination of kinetic parameters of apolipoprotein B metabolism using amino acids labeled with stable isotopes. *J. Lipid Res.* **32:** 1311–1323.
33. Laemmli, U. K. 1970. Cleavage of structural proteins during the assembly of the head of bacteriophage T4. *Nature.* **227:** 680–685.
34. Schwarz, H. P., I. E. Karl, and D. M. Bier. 1980. The alpha-keto acids branched-chain amino acids: simplified derivatization for physiological samples and complete separation as quinoxalinols by packed column gas chromatography. *Anal. Biochem.* **108:** 360–366.
35. Matthews, D. E., E. Ben-Galim, and D. M. Bier. 1979. Determination of stable isotopic enrichment in individual plasma amino acids by chemical ionization mass spectrometry. *Anal. Chem.* **51:** 80–84.
36. Cobelli, C., G. Toffolo, D. M. Bier, and R. Nosadini. 1987. Models to interpret kinetic data in stable isotope tracer studies. *Am. J. Physiol.* **253:** E551–E564.
37. Schonfeld, G., R. S. Lees, P. K. George, and B. Pfleger. 1974. Assay of total plasma apolipoprotein B concentration in human subjects. *J. Clin. Invest.* **53:** 1458–1467.
38. Berman, M., M. Hall, R. I. Levy, S. Eisenberg, D. W. Bilheimer, R. D. Phair, and R. H. Goebel. 1978. Metabolism of apoB and apoC lipoproteins in man: kinetic studies in normal and hyperlipidemic subjects. *J. Lipid Res.* **19:** 38–56.
39. Kesaniemi, Y. A., G. L. Vega, and S. M. Grundy. 1982. Kinetics of apolipoprotein B in normal and hyperlipidemic man: review of current data. *In Lipoprotein Kinetics and Modeling.* Berman, M., S. M. Grundy, and B. V. Howard, editors. Academic Press, New York. 181–205.
40. Packard, C. J., A. Munro, A. R. Lorimer, A. M. Gotto, and J. Shepard. 1984. Metabolism of apolipoprotein B in large triglyceride-rich very low density lipoproteins of normal and hypertriglyceridemic subjects. *J. Clin. Invest.* **74:** 2178–2192.
41. Beltz, W. F., Y. A. Kesaeniemi, B. V. Howard, and S. M. Grundy. 1985. Development of an integrated model for analysis of the kinetics of apolipoprotein B in plasma very low density lipoproteins, intermediate density lipoproteins, and low density lipoproteins. *J. Clin. Invest.* **76:** 575–585.
42. Foster, B. M., R. L. Aamodt, R. I. Henkin, and M. Berman. 1979. Zinc metabolism in humans: a kinetic model. *Am. J. Physiol.* **237:** R340–R349.
43. Berman, M. 1978. SAAM Manual. DHEW Publ. No-NIH 78-180: 1–196.
44. Krul, E. S., Y. Kleinman, M. Kinoshita, B. Pfleger, K. Oida, A. Law, J. Scott, R. Pease, and G. Schonfeld. 1988. Regional specificities of monoclonal anti-human apolipoprotein B antibodies. *J. Lipid Res.* **29:** 937–948.
45. Kane, J. P., D. A. Hardman, and H. E. Paulus. 1980. Heterogeneity of apolipoprotein B: isolation of a new species from human chylomicrons. *Proc. Natl. Acad. Sci. USA.* **77:** 2465–2469.
46. Chuck, S. L., Z. Yao, B. D. Blackhart, B. J. McCarthy, and V. R. Lingappa. 1990. New variations on the translocation of proteins during early biogenesis of apolipoprotein B. *Nature.* **346:** 382–385.
47. Hardman, D. A., C. R. Pullinger, R. L. Hamilton, J. P. Kane, and M. J. Malloy. 1991. Molecular and metabolic basis for the metabolic disorder normotriglyceridemic abetalipoproteinemia. *J. Clin. Invest.* **88:** 1722–1729.
48. Poapst, M., K. Uffelman, and G. Steiner. 1987. The chromogenicity and quantitation of apoB-100 and apoB-48 of human plasma lipoproteins on analytical SDS gel electrophoresis. *Atherosclerosis.* **65:** 75–88.
49. Sato, R., I. Tsuneo, A. Takatsuki, and T. Takano. 1990. Degradation of newly synthesized apolipoprotein B-100 in a pre-Golgi compartment. *J. Biol. Chem.* **265:** 11880–11884.
50. Borèn, J., M. Wetteston, A. Sjöberg, T. Thorlin, G. Bondjers, O. Wiklund, and S-O. Olofsson. 1990. The assembly and secretion of apoB-100 lipoproteins in HepG2 cells. Evidence for different sites for protein synthesis and lipoprotein assembly. *J. Biol. Chem.* **265:** 10556–10564.
51. Chappell, D. A., G. L. Fry, M. A. Waknitz, and J. J. Berns. 1991. Ligand size as a determinant for catabolism by the low density lipoprotein (LDL) receptor pathway. A lattice model for LDL binding. *J. Biol. Chem.* **266:** 19296–19302.